

*Platinum-Palladium Prints at the Nanoscale*

Matthew L. Clarke, Keana Scott, and Alline Myers

The color of platinum-palladium prints can range from neutral to sepia, and can be controlled by managing the relative humidity (RH) during the printing process. The tonal appearance of prints made with the modern ammonium process, which employs ammonium ferric oxalate in the sensitizer, is particularly influenced by humidity. Unlike the traditional process, which employs ferric oxalate in the sensitizer and requires chemical development, the ammonium process requires only water to complete the formation of the platinum-palladium image.<sup>1</sup> Prints made by the ammonium process were the subject of this study.

To adjust the image hue of the print, the sensitized paper may be equilibrated to a specific moisture content immediately before exposure to light through the negative. If enough water is present in the paper to allow ion transport, this soluble ferro-oxalate photoproduct can react to form the metal image during exposure. Drier paper yields warmer tones, but the partially printed-out image must be exposed to moisture, such as by gentle steaming, to finish the printing (fig. 1).

To determine if this difference in tonal appearance is due to different ratios of platinum and palladium depositing at higher RH or if the RH influences the deposited metal particle size, a set of 1:1 platinum:palladium (molar ratio) prints were prepared at 15%, 56% and 85% RH, giving the final prints tones ranging from warm brown to neutral black. X-ray fluorescence (XRF) analysis of these prints across the density steps reveals that the ratio of platinum and palladium metals remains the same regardless of RH (fig. 2). The same trends of increasing metal density with greater light exposure are observed for each step-tablet.

To help explain the differences in color, the prints were investigated by high-resolution electron microscopy to determine the sizes and shapes of the particles that constitute the images. Focused ion beam (FIB) milling was used to prepare thin specimens for analysis (fig. 3).<sup>2</sup> These samples were about 6  $\mu\text{m}$  deep, the depth at which much of the image material resides.<sup>3</sup> The specimens were analyzed by scanning transmission electron microscopy (STEM) and energy dispersive x-ray spectroscopy (EDS). These

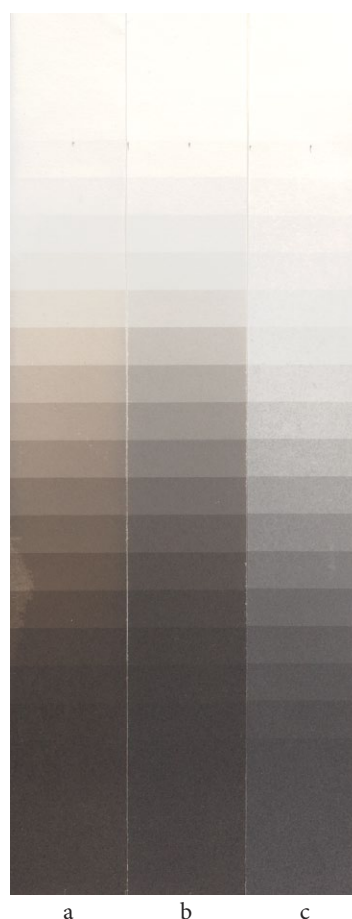


Figure 1. Platinum-palladium step-tablets prepared at the National Gallery of Art by the modern ammonium printing process under different relative humidity: (a) 15% RH, (b) 56% RH, and (c) 85% RH. Exposure time and RH increase from top to bottom and left to right, respectively. Dry paper during exposure yields a warmer-toned print, while humid conditions give neutral tones.

techniques allow for visualization of the nanometer-size particles on the surface and within the cellulose fibers.

All three print samples (conditioned to 15%, 56%, and 85% RH prior to exposure) exhibit particulates consisting of platinum and palladium at the paper surface (fig. 4). These generally appear spherical in shape and have a size on the order of 100 nm. At high resolution it is observed that these particulates are made from small crystalline structures (fig. 5). Within the paper fibers the particle size is dependent on the printing conditions (fig. 6). Specifically, it is shown that at low RH there is a high density of smaller particles. The shape of these oblong particles ( $\approx 10$  nm) may be the result of their formation within the constraints of the fiber structure. As the RH increases, the size of the particulates increases while the overall number of particles falls.

These findings match with the expectation for the formation of nanoparticles. At low RH there is insufficient water to allow the photoexcited iron(II) product to migrate. Therefore, the printing cannot proceed until humidity is introduced in the development process (e.g., steaming) at which time it occurs rapidly, yielding smaller particulates distributed through the cotton fiber. Conversely, high humidity during exposure permits the photoproducts to migrate, allowing the reactions to occur slowly during printing and thus causing the growth of larger particulates. Smaller nanoparticles of platinum and palladium would be predicted to yield browner tones, and larger particles would appear blacker,<sup>4</sup> as the absorbance of these nanoparticles changes due to their size and aggregation.<sup>5</sup> This phenomenon is similarly observed in silver prints with a wider range of color.<sup>6</sup>

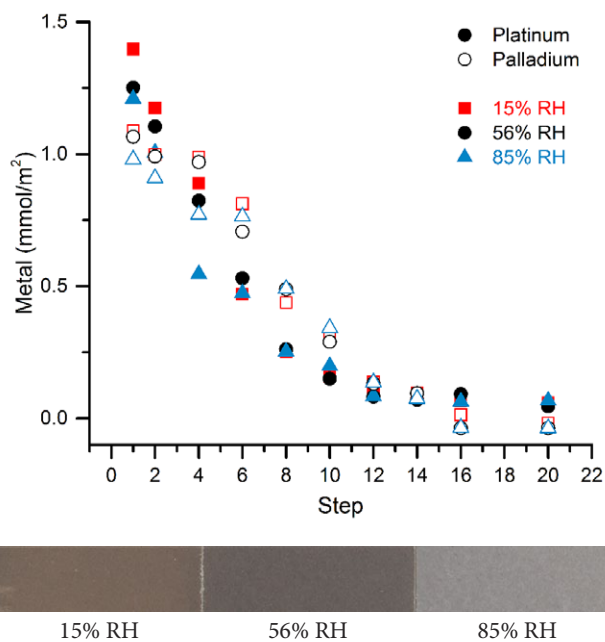
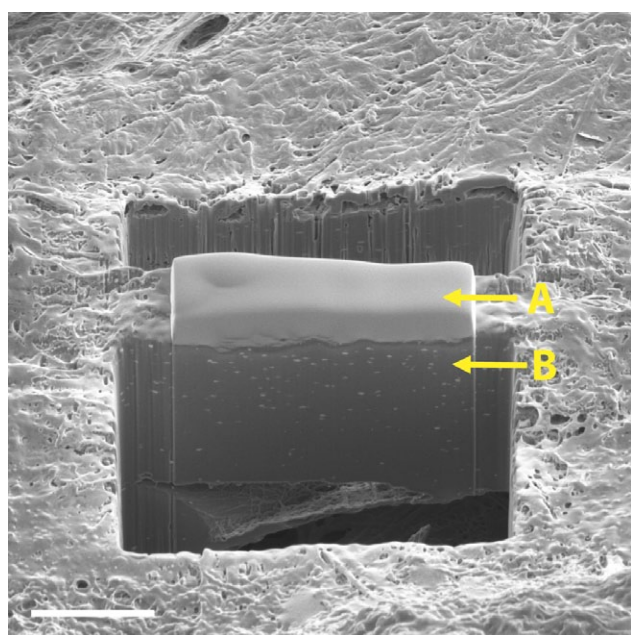
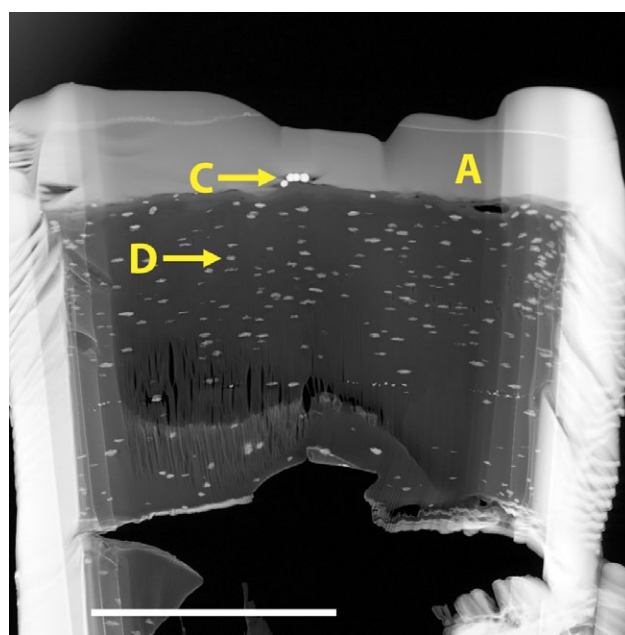


Figure 2. Graph plotting XRF measurements of the molar coating weight of each precious metal as a function of the step-tablets shown in figure 1. Pt and Pd loadings in mmol/m<sup>2</sup> are shown by filled and open symbols, respectively, with the color indicating the % RH, as indicated in the figure legend. For reference, the tones of the step-tablets at step 6 are shown below the graph. Within the measured uncertainty, it is apparent that for a given step the RH does not change the amount of platinum and palladium printed.



3a



3b

Figure 3. An excised portion of a platinum-palladium print milled by FIB for analysis. A layer of carbon (A) was deposited on the surface as a protecting layer (3a). The resulting section (B) was removed, thinned, and viewed by STEM (3b). In 3b, the carbon layer is observed at the top. Large platinum-palladium particles (C) rest at the paper surface, with smaller particles (D) residing within the paper.

3a. Milled print surface with deposit of carbon. Scale bar = 5  $\mu$ m.

3b. Section viewed by STEM. Scale bar = 5  $\mu$ m.

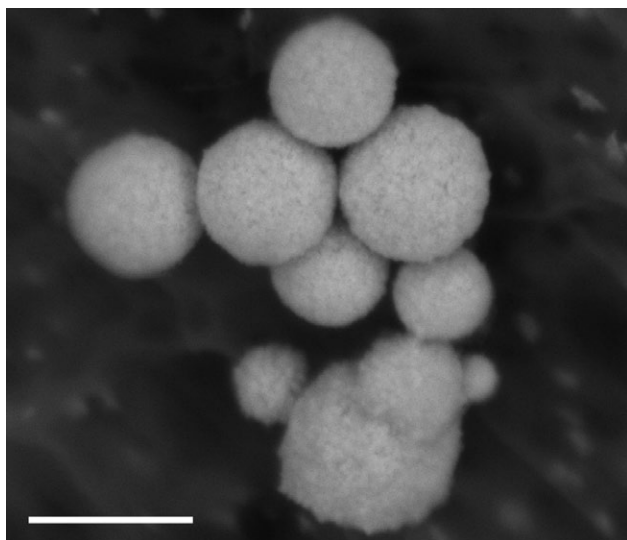


Figure 4. A representative SEM image of the large particulates on the print surface. The white spherical particulates comprise smaller crystals containing both platinum and palladium (as confirmed by EDS). Scale bar = 200 nm.

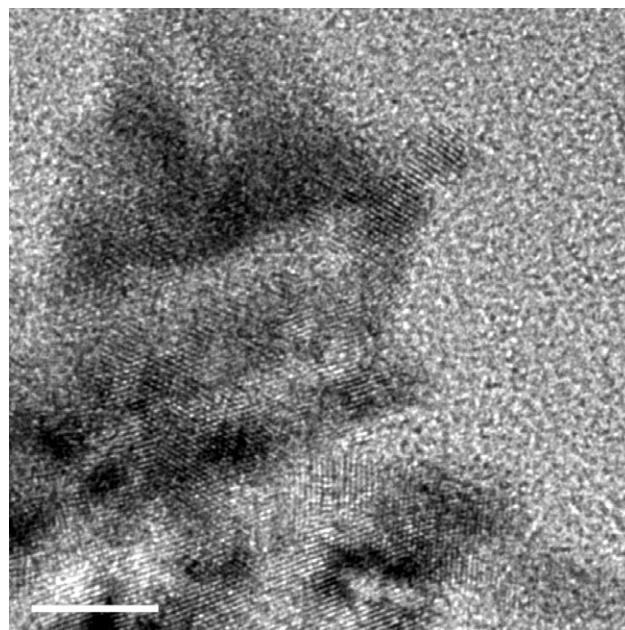


Figure 5. High-resolution STEM image revealing the lattice fringes from the individual platinum-palladium crystals. Scale bar = 2 nm.

## Notes

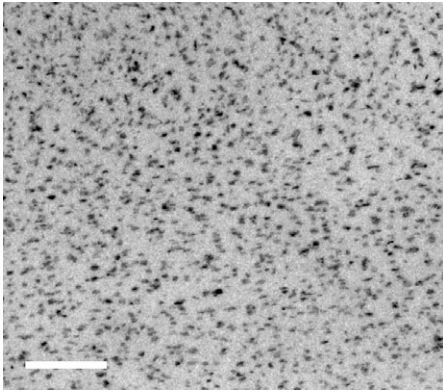
1. Ware 1986.
2. For SEM images and scanning transmission electron microscope (STEM) specimen preparation of the prints, a FEI Helios NanoLab 650 focused ion beam scanning electron microscope (FIB-SEM) was used. Most of the SEM images were collected using a through-the-lens detector (TLD) in the backscattered electron (BSE) mode. STEM specimens were prepared from the print samples using the procedure described in Scott and Giannuzzi 2015. For STEM images of the print specimens, a FEI Titan 80-300 STEM equipped with Gatan Orius 830 CCD camera, operating at 300 kV, was used. In this essay, certain commercial entities, equipment, and materials are identified in order to describe an experimental procedure or concept adequately. Such identification is not intended to imply recommendation or endorsement by the National Institute of Standards and Technology, nor is it intended to imply that the entities, equipment, and materials are necessarily the best available for the purpose.
3. See Matthew L. Clarke, "Characterization, Degradation, and Analysis of Platinum and Palladium Prints," and Patrick Ravines, Natasha Erdman, and Rob McElroy, "The Surface and Subsurface of a Historic Platinum Print," in this volume.
4. Kim et al. 2010.
5. Quinten 2010, 140–41.
6. Mees 1942, 563–68; Ware 1994.

## References

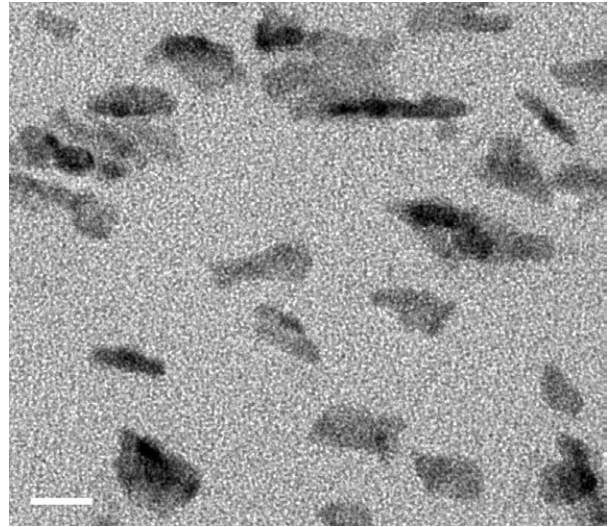
- Kim et al. 2010 Kim, Kwan, Kyung Lock Kim, Hyang Bong Lee, and Kuan Soo Shin. "Surface-Enhanced Raman Scattering on Aggregates of Platinum Nanoparticles with Definite Size." *Journal of Physical Chemistry C* 114 (2010): 18679–85.
- Mees 1942 Mees, C. E. Kenneth. *The Theory of the Photographic Process*. New York: Macmillan, 1942.
- Quinten 2010 Quinten, Michael. *Optical Properties of Nanoparticle Systems: Mie and Beyond*. Weinheim, Germany: Wiley-VCH, 2010.
- Scott and Giannuzzi 2015 Scott, Keana, and Lucille A. Giannuzzi. "Strategies for Transmission Electron Microscopy Specimen Preparation of Polymer Composite." *National Institute of Standards and Technology Special Publication* 1200-16 (September 16, 2015). Online at <http://dx.doi.org/10.6028/NIST.SP.1200-16>.
- Ware 1986 Ware, Michael J. "An Investigation of Platinum and Palladium Printing." *Journal of Photographic Science* 34 (1986): 165–77.
- Ware 1994 Ware, Mike. *Mechanisms of Image Deterioration in Early Photographs: The Sensitivity to Light of W.H.F. Talbot's Halide-Fixed Images, 1834–1844*. Bradford, UK: Science Museum and National Museum of Photography, Film and Television, 1994.

Figure 6. STEM images indicating that within the cellulose fibers the size of the particulates formed is dependent on the RH during exposure. At low RH there is a high density of small particles (6a, 6d). At high RH, larger particulates are observed (6c, 6f).

15% RH

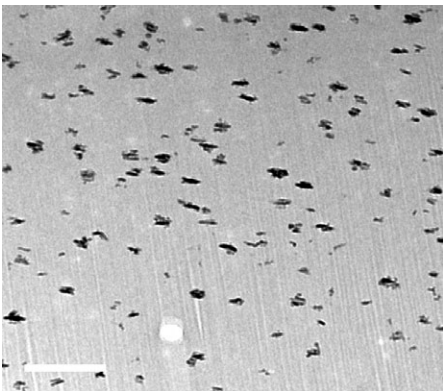


6a. 15% RH. Scale bar = 200 nm.

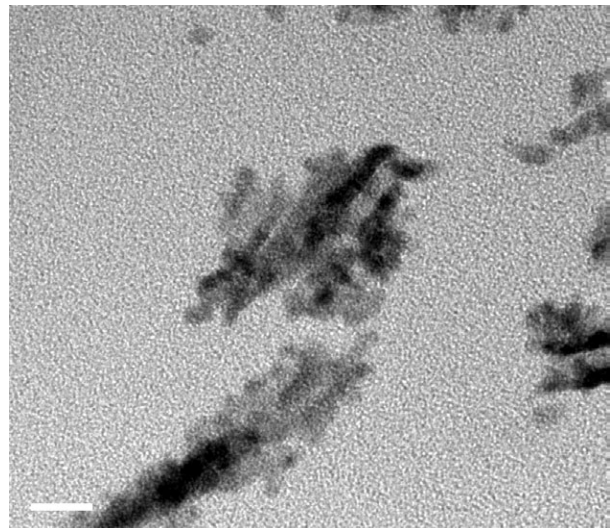


6d. 15% RH. Scale bar = 10 nm.

56% RH

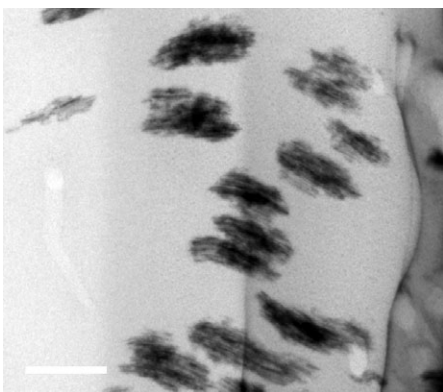


6b. 56% RH. Scale bar = 200 nm.

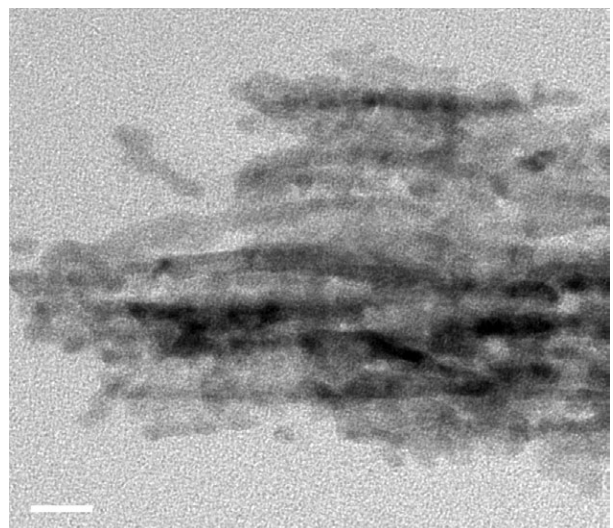


6e. 56% RH. Scale bar = 10 nm.

85% RH



6c. 85% RH. Scale bar = 200 nm.



6f. 85% RH. Scale bar = 10 nm.